# THREE-DIMENSIONAL WAVELET TRANSFORM IN MULTI-DIMENSIONAL BIOMEDICAL VOLUME PROCESSING

Aleš Procházka and Lucie Gráfová
Department of Computing and Control Engineering
Institute of Chemical Technology in Prague
Technická 6, 166 28 Prague 6, Czech Republic
Email: A.Prochazka@ieee.org

Oldřich Vyšata
Neurocenter Caregroup
Jiráskova 1389, 516 01 Rychnov nad Kněžnou
Czech Republic
Email: vysata@neurol.cz

**ABSTRACT**
Object detection and recognition is a common problem related to fault diagnosis in engineering or analysis of changes in biomedical data observations. As such data are often contaminated by noise it is necessary to reduce its effect during this process as well. The paper presents the application of wavelet transform to perform these task using the three dimensional wavelet decomposition, coefficients thresholding and object reconstruction. The proposed method is verified for simulated data at first and then applied for processing of backbone parts to emphasize its selected components. The goal of the paper is in (i) the presentation of the three-dimensional wavelet transform, (ii) discussion of its use for volume data de-nosing, and (iii) proposal of the following data extraction to allow their classification. The paper compares numerical results achieved by the use of different wavelet functions and thresholding methods with the experience of an expert to propose the best algorithmic approach to this problem.

**KEY WORDS**
Multi-dimensional signal proceesing, volume data analysis, discrete wavelet transform, object decomposition and reconstruction, coefficients thresholding, biomedical data enhancement

## 1 Introduction

Multi-dimensional data analysis [29, 28] and multi-resolution modelling form a specific area of digital signal processing with many interdisciplinary applications having the common mathematical background. The interest in this area is closely connected with the three-dimensional modelling and visualization.

The main goal of the paper is to show the de-noising algorithms based upon the discrete wavelet transform (DWT) that can be applied successfully to enhance noisy multidimensional magnetic resonance (MR) data sets including the two-dimensional (2-D) image slices and three-dimensional (3-D) image volumes. Noise removal or de-noising is an important task in image processing used to recover a volume data that has been corrupted by noise.

Main topics discussed include the visualization of 2-D MR slices and 3-D image volumes. The application of the proposed algorithms is mainly in the area of magnetic resonance imaging (MRI) as an imaging technique used primarily in medical field [14, 12] to produce high quality images of the soft tissues of the human body. An insight to the visualization of MRI data sets i.e. 2-D image slices or 3-D image volumes is of paramount importance to the medical doctors.

Fig. 1 presents an example of such data allowing to study selected vertebrae slices and to separate its anatomic components [3, 5, 32, 15] together with the analysis of their structure, sizes and positions. Mathematical methods discussed further are used (i) to enhance such data and (ii) to find information important for the appropriate treatment.

The discrete wavelet transform [6, 27, 20, 23] plays an increasingly important role in the de-noising of MR images. The three-dimensional (3-D) digital image processing, and in particular 3-D DWT, is a rapidly developing research area with applications in many scientific fields such as biomedicine, seismology, remote sensing, material science, etc [19]. The 3-D DWT algorithms are implemented as an extension of the existing 2-D algorithms. The performance of the de-noising algorithms are quantitatively assessed using different criteria namely the mean square error (MSE), peak signal-to-noise ratio (PSNR) and the visual appearance. The results are discussed in accordance to the type of noise and wavelets implemented.

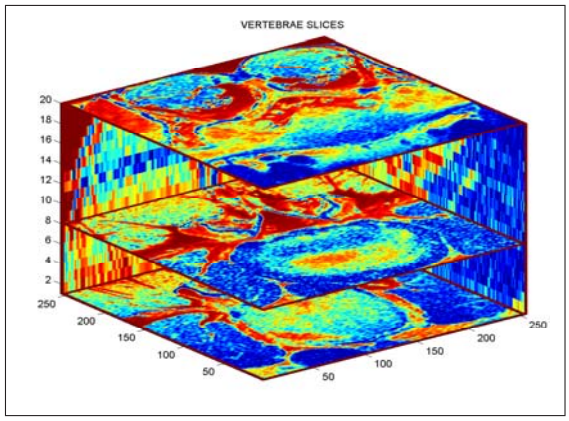


Figure 1. Selected vertebrae slices and the three-dimensional visualization of the backbone region

## 2 Three-Dimensional Wavelet Decomposition

Wavelet transform [6, 24, 27, 20] provides mathematical tools for time-scale signal analysis in the similar way as the short time Fourier transform (STFT) in the time-frequency domain. The main difference is in the use of time limited analysing wavelet functions allowing different scale resolution for dilated initial wavelet. Wavelet series constructed with two parameters, scale and translation, provide in this way the ability to zoom in on the transient behavior of the signal. The continuous wavelet transform [16] is defined as the convolution of $x(t)$ with a wavelet function, $W(t)$, shifted in time by a translation parameter $b$ and a dilation parameter $a$ (Eq. (1))

$$X_W(a,b) = \frac{1}{\sqrt{a}} \int_{-\infty}^{\infty} W\left(\frac{t-b}{a}\right) x(t)dt \qquad (1)$$

The discrete form of the wavelet transform is based upon the discretization of parameters $(a, b)$ on the time-scale plane corresponding to a discrete set of continuous basis functions. This can be achieved defining

$$W_{j,k}(t) = \frac{1}{\sqrt{a_j}}\, W\left(\frac{t-b_k}{a_j}\right) \qquad (2)$$

for $a_j = a_0^j$ and $b_k = kb_0a_0^j$ where $j, k \in Z, \quad a_0 > 1, \quad b_0 \neq 0$ where $j$ controls the dilation and $k$ controls the translation. Two popular choices for the discrete wavelet parameters $a_0$ and $b_0$ are 2 and 1 respectively, a configuration that is known as the *dyadic grid* arrangement resulting in

$$\begin{aligned} W_{j,k}(t) &= a_0^{-j/2}\ W(a_0^{-j}\ t - kb_0) \\ &= 2^{-j/2}\ W(2^{-j}\ t - k) \end{aligned}$$

Wavelet analysis is simply the process of decomposing a signal into shifted and scaled versions of a mother (initial) wavelet. An important property of wavelet analysis is perfect reconstruction, which is the process of reassembling a decomposed signal or image into its original form without loss of information. For decomposition and reconstruction the scaling function $\Phi_{jk}(t)$ and the wavelet $W_{jk}(t)$ are used in the form

$$\Phi_{jk}(t) = 2^{-\frac{j}{2}}\ \Phi_0(2^{-j}\ t - k) \qquad (3)$$

$$W_{jk}(t) = 2^{-\frac{j}{2}}\ \Psi_0(2^{-j}\ t - k) \qquad (4)$$

where $m$ stands for dilation or compression and $k$ is the translation index. Every basis function $W$ is orthogonal to every basis function $\Phi$.

The one-dimensional wavelet transform of a discrete-time signal $x(n)$ $(n = 0, 1, \ldots, N)$ is performed by convolving signal $x(n)$ with both a half-band low-pass filter $L$ and high-pass filter $H$ and downsampling by two.

$$c(n) = \sum_{n=0}^{L-1} h_0(k)\ x(n-k) \qquad d(n) = \sum_{n=0}^{L-1} h_1(k)\ x(n-k) \qquad (5)$$

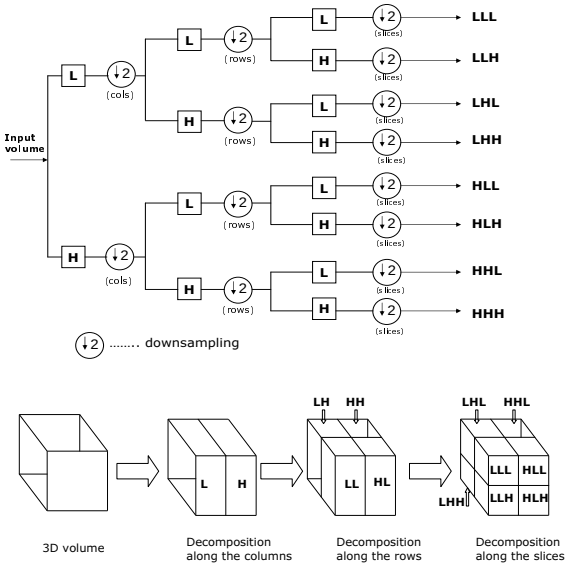


Figure 2. The decomposition tree of the three-dimensional volume decomposition using discrete wavelet transform for columns rows and slices producing 8 subvolumes in the first decomposition stage

where $c(n)$ represent the approximation coefficients for $n = 0, 1, 2 \ldots, N-1$ and $d(n)$ are the detail coefficients, $h_0$ and $h_1$ , are coefficients of the discrete-time filters $L$ and $H$ respectively

$$\{h_0(n)\}_{n=0}^{L-1} = (h_0(0),\ h_0(1),\ \ldots,\ h_0(L-1)) \qquad (6)$$

$$\{h_1(n)\}_{n=0}^{L-1} = (h_1(0),\ h_1(1),\ \ldots,\ h_1(L-1)) \qquad (7)$$

resulting in the separable, sub-band process.

Similar decomposition process can be applied for multi-dimensional signals. The three-dimensional wavelets [28, 26, 14, 18] can be constructed as separable products of 1-D wavelets by successively applying a 1-D analyzing wavelet in three spatial directions $(x, y, z)$. Fig. 2 shows a one-level separable 3-D discrete wavelet decomposition [27] of an image volume. The volume $F(x, y, z)$ is firstly filtered along the $x$-dimension, resulting in a low-pass image $L(x, y, z)$ and a high-pass image $H(x, y, z)$. Both $L$ and $H$ are then filtered along the $y$-dimension, resulting in four decomposed sub-volumes: $LL$, $LH$, $HL$ and $HH$. Then each of these four subvolumes are filtered along the $z$-dimension, resulting in eight sub-volumes: *LLL, LLH, LHL, LHH, HLL, HLH, HHL* and *HHH* .

The reduction of noise present in images is an important aspect of image processing. De-noising is a procedure to recover a signal that has been corrupted by noise. After discrete wavelet decomposition the resulting coefficients can be modified to eliminate undesirable signal components. To implement wavelet thresholding a *wavelet shrinkage* method for de-noising the image has been verified. The proposed algorithm to be used consists of the following steps:

Algorithm A: Wavelet image de-noising

- Choice of a wavelet (e.g. Haar, symmlet, etc) and number of levels or scales for the decomposition. Computation of the forward wavelet transform of the noisy image
- Estimation of a threshold
- Choice of a shrinkage rule and application of the threshold to the detail coefficients. This can be accomplished by *hard* or *soft* thresholding
- Application of the inverse transform (wavelet reconstruction) using the modified (thresholded) coefficients

Thresholding is a technique used for signal and image de-noising. The shrinkage rule define how we apply the threshold. There are two main approaches which are:

- Hard thresholding deletes all coefficients that are smaller than the threshold $\lambda$ and keeps the others unchanged. The hard thresholding is defined by relation

$$\bar{c}_s(k) = \begin{cases} \text{sign } c(k)\ (|c(k)|) & \text{if } |c(k)| > \lambda \\ 0 & \text{if } |c(k)| \leq \lambda \end{cases} \quad (8)$$

  where $\lambda$ is the threshold and the coefficients that are above the threshold are the only ones to be considered. The coefficients whose absolute values are lower than the threshold are set to zero.

- Soft thresholding deletes the coefficients under the threshold, but scales the ones that are left. The general soft shrinkage rule is defined relation

$$\bar{c}_s(k) = \begin{cases} \text{sign } c(k)\ (|c(k)| - \lambda) & \text{if } |c(k)| > \lambda \\ 0 & \text{if } |c(k)| \leq \lambda \end{cases} \quad (9)$$

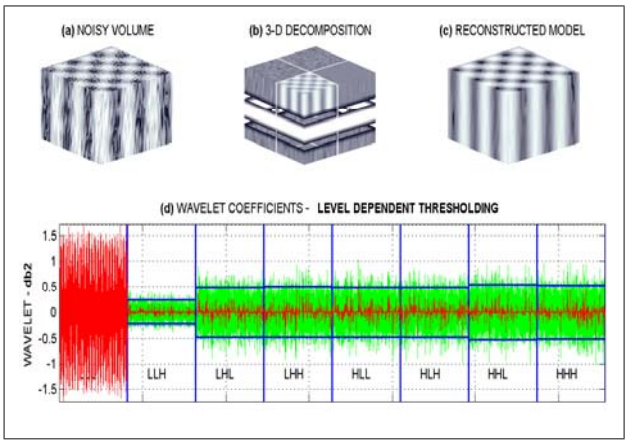


Figure 3. The noisy volume processing including **(a)** simulated noisy data, **(b)** volume decomposition into the first stage, **(d)** ordered wavelet coefficients and their local thresholding values, and **(c )** the reconstructed body

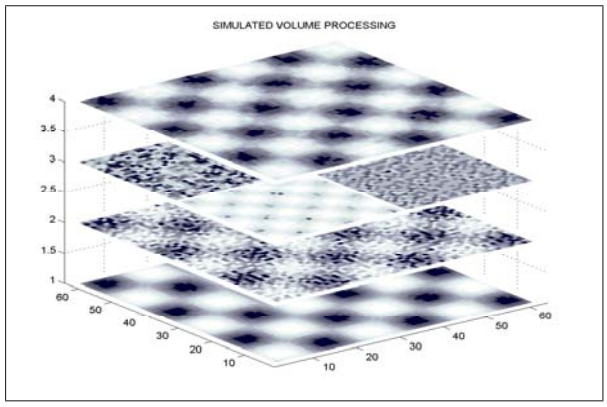


Figure 4. Data processing presenting from the bottom to the top **(1)** simulated slice, **(2)** noisy slice, **(3)** decomposed slice, and **(4)** the reconstructed slice after noise rejection

Results of this process applied for a simulated noisy volume processing is presented in Fig. 3. Threshold limits are estimated separately for each subvolume coefficients [30] using a specific algorithm based upon values of wavelet coefficients.

Fig. 4 presents the whole process for a selected volume slice starting with the simulated volume and resulting in its reconstruction after the decomposition into the first level. Fig. 5 presents selected first volume slice contours. The compressed $LLL$ subvolume can be used in the next stage to evaluate its 8 subvolumes again.

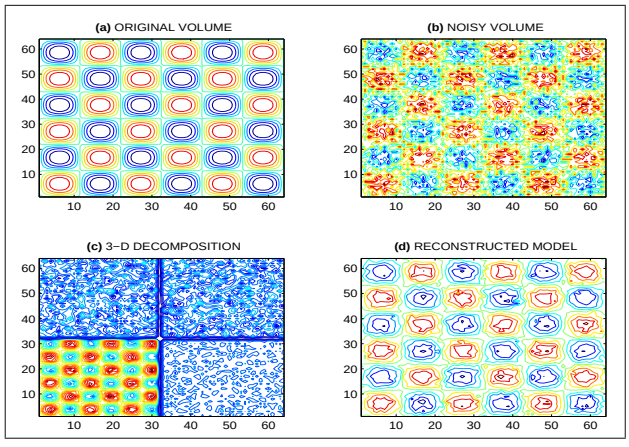


Figure 5. Contour values of the first slice presenting **(a)** simulated data formed by harmonic functions, **(b)** noisy slice, **(c)** decomposed slice for the first decomposition stage, and **(d)** the reconstructed slice

## 3 Backbone Volume De-Noising

Biomedical image processing and volumetric data registration forms an extensive research area with many applications [8, 4, 25, 10, 7, 11, 9, 22]. Fig. 6(a) presents an example of vertebrae volume data used for diagnostical purposes and detection of medical problems.

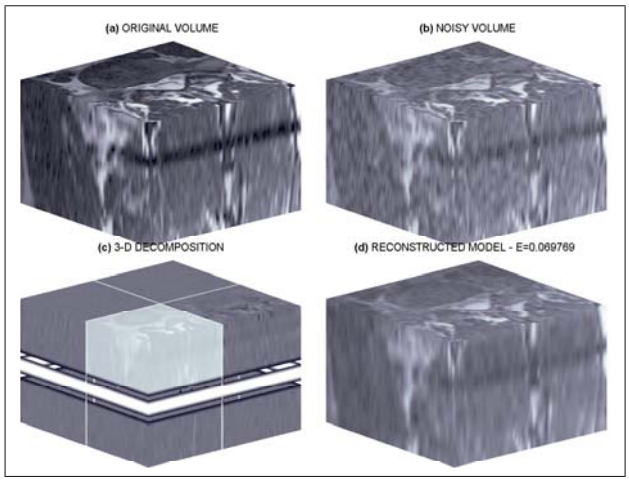


Figure 6. Volume data processing presenting **(a)** real part of the backbone area for a vertebrae study, **(b)** noisy volume, **(c)** decomposed subvolumes, and **(d)** the reconstructed data after noise rejection

The initial stage of such data processing includes image de-nosing [31, 2, 17] for artifacts rejection. Fig. 7 presents the typical noise analysis using MRI data subvolume selected from area outside the observed body. To study the effect of real data de-nosing the similar noise has been added to real data and the three dimensional wavelet transform with different wavelet functions for volume denoising has been applied using median estimates of threshold values. Further possibilities include their adaptive modification [33].

Fig. 6 compares the vertebrae volume before and after de-noising using db4 wavelet function with contours of the first slice in Fig. 8 allowing numerical comparison of original and processed data.

Table 1 presents analysis of the use of different wavelet functions and both local and global thresholding approach. Resulting sum of squared differences between evaluated and original values provides the comparison between selected wavelet functions and presents the efficiency of Haar wavelet function in this case.

## 4 Volume Components Detection

Volume components extraction of the vertebrae data form the main processing goal to enable precise diagnosis and treatment. The study is based on fundamental data segmentation [13, 1] including classical image processing methods [21] using thresholding and watershed transform to distinguish the bone, soft tissue, fat and further elements. Fig. 9

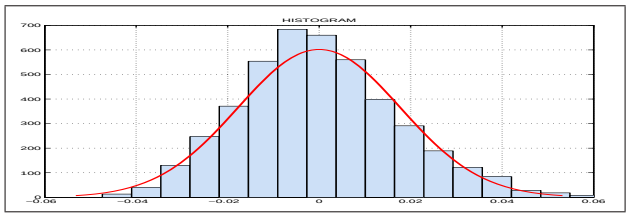


Figure 7. Histogram of the real noise in the volumetric vertebrae data

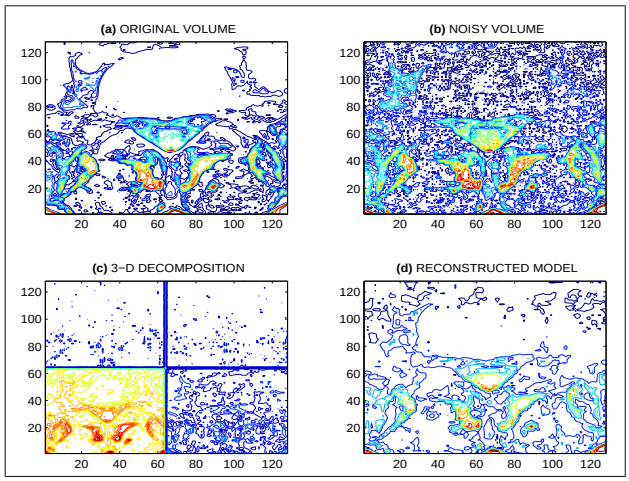


Figure 8. Contour values of the first vertebrae slice presenting **(a)** real data, **(b)** noisy slice, **(c)** decomposed slice for the first decomposition stage, and **(d)** the reconstructed vertebrae slice

Table 1. WAVELET FUNCTION USE FOR MRI DATA DENOISING COMPARING ORIGINAL AND RECONSTRUCTED VOLUMES FOR DIFFERENT KINDS OF THRESHOLDING

| Method | | Error Value | | |
|---|---|---|---|---|
| *Thresholding method* | *Wavelet function* | *Set 1* | *Set 2* | *Set 3* |
| *Local* | haar | 0.071 | 0.079 | 0.040 |
| | db2 | 0.105 | 0.105 | 0.070 |
| | db4 | 0.089 | 0.080 | 0.052 |
| | sym2 | 0.105 | 0.105 | 0.070 |
| | sym4 | 0.071 | 0.107 | 0.057 |
| *Global* | haar | 0.063 | 0.102 | 0.042 |
| | db2 | 0.120 | 0.113 | 0.068 |
| | db4 | 0.084 | 0.090 | 0.064 |
| | sym2 | 0.120 | 0.113 | 0.068 |
| | sym4 | 0.084 | 0.090 | 0.060 |

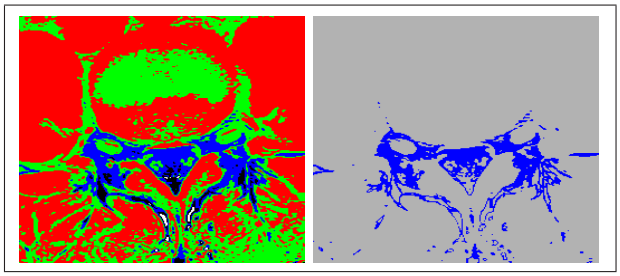

Figure 9. A selected vertebra slice (on the left) and extraction of selected objects (on the right)

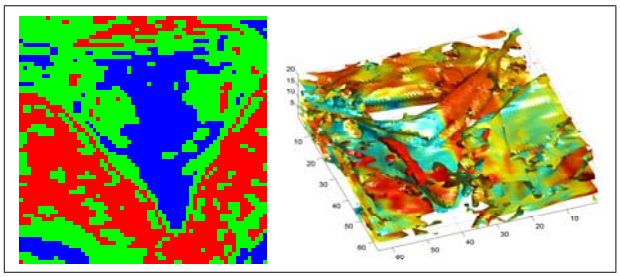

Figure 10. A selected vertebra slice part (on the left) and its three-dimensional volume visualization (on the right)

presents the selected vertebrae slice with an extracted image component and its detail in Fig. 10.

For classification of volumetric segments it is necessary to find their characteristic features. The preliminary studies proved the possibility to use wavelet decomposition again to detect texture complexity and its energy distribution. The following algorithm specify such an approach for each volumetric segment found.

Algorithm B: Feature extraction

- Application of the wavelet transform for a selected wavelet and decomposition level
- Calculation of the energy inside the image detail subband
- Selection of energy components to form the feature vector

Feature vectors can then be classified into the given number of classes using selected clustering methods including neural networks as well.

## 5 Conclusion

The paper forms a contribution to the three-dimensional wavelet transform use for the analysis of the vertebrae volume. The general method of the multi-resolution volume decomposition and reconstruction combined with wavelet coefficients thresholding has been applied for volumetric data de-nosing at first.

Volume elements segmentation and classification is mentioned further in connection with wavelet transform use for feature extraction. Resulting algorithms have been used to compare different wavelet functions for rejection of additional noise and proposed methods were then applied for real volumetric data processing to extract their components necessary for a proper analysis, diagnosis and medical treatment.

The following work will be devoted to the three-dimensional separation of biomedical volume structures to contribute to the more precise detection of anatomic disorders and proposal of their correction using appropriate visualisation methods including the medical virtual reality tools.

Further mathematical analysis will be devoted to complex wavelet transform use, statistical models, 3D registration, segmentation and visualization in connection with the detail physiological interpretation of results.

## Acknowledgement

Real MRI data have been kindly provided by the Neurocenter Caregroup in Rychnov nad Kněžnou and the paper has been supported by the Research grant No. MSM 6046137306.

## References

[1] M. S. Aslan, A. Ali, B. Arnold H. Rara and, R. Fahmi, A. A. Farag, and P. Xiang. A Novel, Fast, and Complete 3D Segmentation of Vertebral Bones. In *The 35th Int. Conference on Acoustics, Speech and Signal Processing(ICASSP 2010)*, pages 654–657, 2010.

[2] S. P. Awate and R. T. Whitaker. Feature-Preserving MRI Denoising: A Nonparametric Empirical-Bayes Approach. *IEEE Trans. Med. Imaging*, 29(9):1242–1255, 2007.

[3] S. Benameura, M. Mignottea, S. Parentd, H. Labelled, W. Skallie, and J. Guisea. 3D/2D registration and segmentation of scoliotic vertebrae using statistical models. *Computerized Medical Imaging and Graphics*, 27:321–337, 2003.

[4] W. Birkfellner, M. Figl, and H. Bergmann. Rigid 2D/3D Slice-to-Volume Registration and its Application on Fluoroscopic CT Images. *Medical Physics*, 34(1):246–255, 2007.

[5] S. Cukovic, G. Devedzic, L. Ivanovic, T. Z. Lukovic, and K. Subburaj. Segmental Assessment and Visualization of Trabecular Bone Mineral Density in Vertebrae. *Computer Aided Design and Applications*, 7(1):153–161, 2010.

[6] I. Daubechies. The Wavelet Transform, Time-Frequency Localization and Signal Analysis. *IEEE Trans. Inform. Theory*, 36:961–1005, Sept. 1990.

[7] B. Fei, J. L. Duerk, D. T. Boll, J. S. Lewin, and D. L.Wilson. Slice-to-Volume Registration and its Potential Application to Interventional MRI-Guided Radio-Frequency Thermal Ablation of Prostate Cancer. *IEEE Transactions on Medical Imaging*, 22(4):515–525, April 2003.

[8] L. Fruhwald, J. Kettenbach, M. Figl, J. Hummel, H. Bergmann, and W. Birkfellner. A Comparative Study on Manual and Automatic Slice-to-volume Registration of CT Images. *European Radiology*, 19(11):2647–2653, 2007.

[9] S. Gefen, L. Bertrand, N. Kiryati, and J. Nissanov. Localization of sections within the brain via 2D to 3D image registration. In *Proceedings of the IEEE International Conference on Acoustics, Speech, and Signal Processing (ICASSP 05)*, volume 2, pages 733–736. IEEE, 2005.

[10] M. Hemmendorff, M. Andersson, T. Kronander, and H. Knutsson. Phase-based Multidimensional Volume Registration. *IEEE Transactions on Medical Imaging*, 21(12):1536–43, December 2002.

[11] M. Holden, D. L. G. Hill, and E. R. E. Denton. Voxel similarity measures for 3-D serial MR brain image registration. *IEEE Transactions on Medical Imaging*, 19(2):94–102, 2000.

[12] Image Processing Toolbox. The Mathworks, Inc., 3 Apple Hill Drive, Natick, Massachusetts, U.S.A., 2010. http://www.mathworks.com/help/pdf_doc/allpdf.html.

[13] Y. Kim and D. Kim. A fully Automatic Vertebra Segmentation Method Using 3D Deformable Fences. *Computerized Medical Imaging and Graphics*, 33(5):343–352, July 2009.

[14] D. Kleut, M. Jovanovic, and B. Reljin. 3D Visualisation of MRI images using MATLAB. *Journal of Automatic Control, University of Belgrade*, 16:1–3, 2006.

[15] D. Létourneau, A. Vloet R. Wong, D. A. Fitzpatrick, and M. Gospodarowicz. Semiautomatic Vertebrae Visualization, Detection, and Identification for Online Palliative Radiotherapy of Bone Metastases of the Spine. *Medical Physics*, 35:367–376, 2008.

[16] Sheng-Tun Li, Shih-Wei Chou, and Jeng-Jong Pan. Multi-Resolution Spatio-Temporal Data Mining for the Study of Air Pollutant Regionalization. In *33rd Annual Hawaii International Conference on System Sciences(HICSS)*, pages 1–7, 2000.

[17] J. V. Manjona, J. Carbonell-Caballeroa, J. J. Lulla, G. Garcia-Martia, Luis Marti-Bonmatib, and M. Robles. MRI Denoising Using Non-Local Means. *Medical Image Analysis*, 12(4):514–523, August 2008.

[18] M. Misiti, Y. Misiti, G. Oppenheim, and J. M. Poggi. *Wavelet Toolbox*. The Mathworks, Inc., 3 Apple Hill Drive, Natick, Massachusetts, U.S.A., 2010. http://www.mathworks.com/help/pdf_doc/allpdf.html.

[19] V. Musoko. *Biomedical Signal and Image Processing*. PhD thesis, Institute of Chemical Technology in Prague, Czech Republic, 2005.

[20] D.E. Newland. *An Introduction to Random Vibrations, Spectral and Wavelet Analysis*. Longman Scientific & Technical, Essex, U.K., third edition, 1994.

[21] M. Nixon and A. Aguado. *Feature Extraction & Image Processing*. Elsevier, Amsterdam, 2004.

[22] S. Osechinskiy and F. Kruggel. Slice-to-Volume Nonrigid Registration of Histological Sections to MR Images of the Human Brain. *Anatomy Research International*, pages 1–17, 2011. ID: 287860.

[23] A. Procházka, J. Jech, and J. Smith. Wavelet Transform Use in Signal Processing. In *31st International Conference in Acoustics*, pages 209–213. Czech Technical University, 1994.

[24] A. Procházka and V. Sýs. Application of Genetic Algorithms for Wavelet Networks Signal Modelling. In *VIIth European Signal Processing Conference EUSIPCO-94*, pages II/1078–II/1081. European Association for Signal Processing, 1994.

[25] C. G. Ravichandran and G. Ravindran. Inter-slice Reconstruction of MRI Image Using One Dimensional Signal Interpolation. *International Journal of Computer Science and Network Security*, 8(10):351–356, October 2008.

[26] E. Schiavi, C. Hernandez, and J. A. Hernandez. Fully 3D Wavelets MRI Compression. In J. M. Barreiro, F. M. Sanchez, V. Maojo, and F. Sanz, editors, *Biological and Medical Data Analysis*, volume 3337 of *Lecture Notes in Computer Science*, pages 9–20. Springer Berlin / Heidelberg, 2004.

[27] I. W. Selesnick, R. G. Baraniuk, and N. G. Kingsbury. The Dual-Tree Complex Wavelet Transform. *IEEE Signal Processing Magazine*, 22(6):123–151, 2005.

[28] N. Sriraam and R. Shyamsunder. 3-D Medical Image Compression Using 3-D Wavelet Coders . *Digital Signal Processing*, 21(1):100–109, January 2011.

[29] B. Starly, Z. Fang, W. Sun, A. Shokoufandeh, and W. Regli. Three-Dimensional Reconstruction for Medical-CAD Modeling. *Computer-Aided Design & Applications*, 3(1–4):431–438, 2005.

[30] G. Strang. Wavelet transforms versus fourier transforms. *American Mathematical Society*, 28(2):228–305, April 1993.

[31] S. V. Vaseghi. *Advanced Digital Signal Processing and Noise Reduction*. John Wiley & Sons Ltd, 2006.

[32] S. Wesarg, A. G. Hosseini, M. Erdt, K. Kafchitsas, and M. Khan. Segmental Assessment and Visualization of Trabecular Bone Mineral Density in Vertebrae. In *Eurographics Workshop on Visual Computing for Biology and Medicine*, pages 1–3. IEEE, 2010.

[33] X. P. Zhang. Thresholding Neural Network for Adaptive Noise Reduction. *IEEE Transastions on Neural Networks*, 12(3):567–584, 2001.